

A WIND TUNNEL INVESTIGATION OF THE INFLUENCE OF SOLAR-INDUCED WALL-HEATING ON THE FLOW REGIME WITHIN A SIMULATED URBAN STREET CANYON

A. KOVAR-PANSKUS¹, L. MOULINNEUF², E. SAVORY^{3*}, A. ABDELQARI²,
J.-F. SINI², J.-M. ROSANT², A. ROBINS¹ and N. TOY¹

¹ *Fluids Research Centre, School of Engineering, University of Surrey, Guildford, Surrey, U.K.;*

² *Ecole Centrale de Nantes, Laboratoire de Mécanique des Fluides, Nantes, Cedex 3, France;*

³ *Department of Mechanical and Materials Engineering, Faculty of Engineering, University of Western Ontario, London, Ontario, Canada*

(* author for correspondence, e-mail: e.savory@eng.uwo.ca, fax: +44 (0) 1483 450984)

Abstract. A wind tunnel study has been undertaken to assess the influence of solar-induced wall heating on the airflow pattern within a street canyon under low-speed wind conditions. This flow is normally dominated by large-scale vortical motion, such that the wind moves downwards at the downstream wall. In the present work the aim has been to examine whether the buoyancy forces generated at this wall by solar-induced heating are of sufficient strength to oppose the downward inertial forces and, thereby, change the canyon flow pattern. Such changes will also influence the dispersion of pollutants within the street. In the experiments the windward-facing wall of a canyon has been uniformly heated to simulate the effect of solar radiation. Four different test cases, representing different degrees of buoyancy (defined by a test Froude number, Fr), have been examined using a simple, 2-D, square-section canyon model in a wind tunnel. For reference purposes, the neutral case (no wall heating), has also been studied. The approach flow boundary layer conditions have been well defined, with the wind normal to the main canyon axis, and measurements have been taken of canyon wall and air temperatures and profiles of mean velocities and turbulence intensities. Analysis of the results shows clear differences in the flow patterns. As Fr decreases from the neutral case there are reductions of up to 50% in the magnitudes of the reverse flow velocities near the ground and in the upward motion near the upstream wall. A marked transition occurs at $Fr \approx 1$, where the single dominant vortex, existing at higher Fr values, weakens and moves upwards whilst a lower region of relatively stagnant flow appears. This transition had previously been observed in numerical model predictions but at a Fr at least an order of magnitude higher.

Keywords: buoyancy, cavity flow, Froude number, street canyon, thermal effects

Nomenclature

d	=	Displacement height	(m)
Fr	=	Froude number	(–)
H, W	=	Height and width of canyon	(m)
k	=	Turbulent kinetic energy	(m ² s ^{–2})
L	=	Spanwise canyon length	(m)



Water, Air, and Soil Pollution: Focus **2**: 555–571, 2002.

© 2002 Kluwer Academic Publishers. Printed in the Netherlands.

Re	=	Reynolds number, $U_{ref} H/\nu$	
T	=	Air temperature	(°C)
T_w	=	Temperature of heated wall	(°C)
T_{ref}	=	Freestream air temperature	(°C)
$\overline{U}, \overline{W}$	=	Mean velocity components	(m s ⁻¹)
U_{ref}	=	Freestream velocity	(m s ⁻¹)
u', w'	=	Rms velocity fluctuations	(m s ⁻¹)
u_*	=	Friction velocity	(m s ⁻¹)
Vel	=	Velocity vector, $(\overline{U}^2 + \overline{W}^2)^{1/2}$	(m s ⁻¹)
X, Y, Z	=	Co-ordinate system	(m)
z_0	=	Roughness length	(m)
δ	=	Boundary layer thickness	(m)
ν	=	Kinematic viscosity of air	(m ² s ⁻¹)

1. Introduction

The wind flow field within urban areas has been studied for several decades, with several investigations of the main flow patterns occurring within street canyons (Albrecht, 1933; followed by Georgii *et al.*, 1967; Ludwig and Dabberdt, 1972; DePaul and Sheih, 1986). All these researchers undertook full-scale measurements in a street canyon, under conditions of the wind perpendicular to the main canyon axis, and observed the main vortex that tends to be established under these wind conditions. Further research focussed on the dependence of the flow patterns and also the dispersion of pollutants on the aspect ratio of the canyon (streamwise width/depth), different roof shapes (Rafailidis, 1997), and the effect of traffic (Vachon, 2000).

Another topic of interest, especially under conditions of low wind speed, is the influence of wall heating in street canyons due to solar radiation incident on one or more walls during the course of a day. Full-scale measurements have been conducted to gain knowledge about the influence of wind speed, temperature, and stability conditions on the canyon flow regime (Nakamura and Oke, 1988; Vachon, 2000), whilst wind tunnel studies investigating the same problems have been conducted by Ogawa *et al.* (1981), and Uehara *et al.* (1997a, 2000). In addition, the dispersion of pollutants has been investigated within street canyons in stratified urban canopy layers (Uehara *et al.*, 1997b). However, the influence of different buoyancy effects due to canyon wall heating has not previously been assessed through wind tunnel simulations under carefully controlled conditions, because it is a challenging problem to match the necessary similarity laws for velocity and temperature via an appropriate Froude number. The effect of wall heating on the flow and pollution dispersion characteristics within the canyon is likely to be

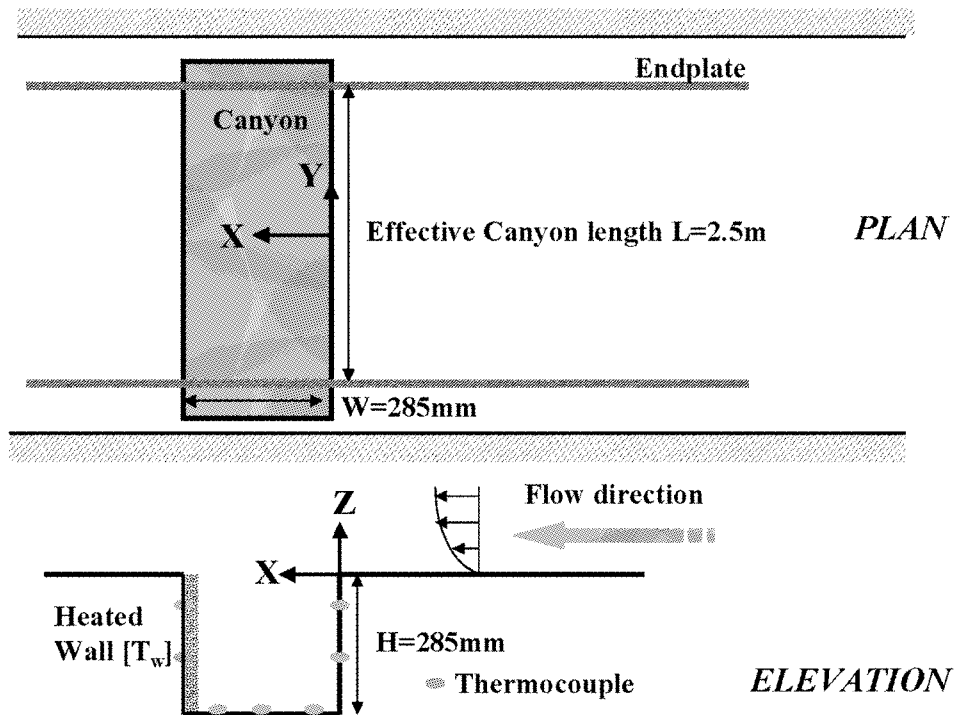


Figure 1. Diagrammatic layout of wind tunnel and canyon model.

greatest when the windward-facing wall is heated. This is because the buoyancy forces generated at that wall by the heating directly oppose the downward inertial forces in the same region that are associated with the dominant canyon vortex. It is anticipated, from previous numerical predictions (Mestayer *et al.*, 1995), that, under certain conditions, the buoyancy forces will be large enough to disrupt the canyon vortex to form a different regime with consequent effects on the local flow and pollutant dispersion characteristics.

This article reports on an initial examination of this complex problem, studying the effect of Froude number on the main flow features in a simple, yet not too unrealistic, 2-D canyon in order to determine the transition conditions between any different regimes and whether there is a threshold Froude number above which such thermal effects may be neglected. A second aim of the work is to provide a detailed data set for developing computational fluid dynamics (CFD) models for predicting these flow regimes.

2. Experimental Details

A comprehensive study was conducted in the EnFlo Laboratory wind tunnel of the Fluids Research Centre at the University of Surrey. A nominally two-dimensional

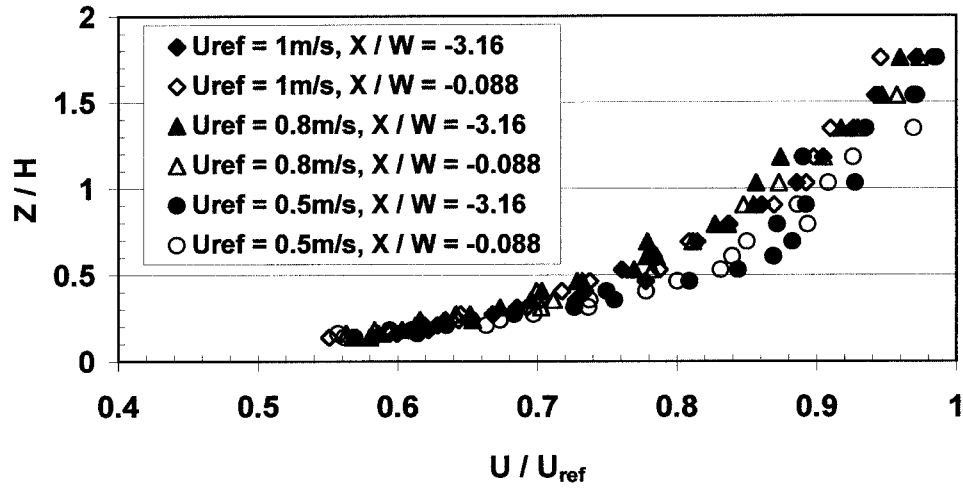


Figure 2. Boundary layer mean velocity profiles for different windspeeds.

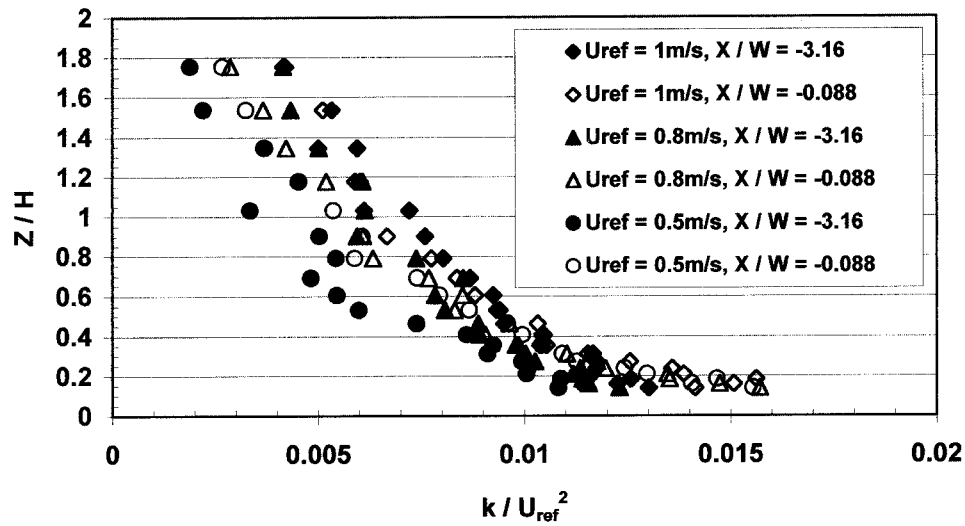


Figure 3. Boundary layer turbulent kinetic energy profiles for different windspeeds.

(2-D), 285 mm square section ($W/H = 1$) cavity of 3 m length was installed with its principal axis perpendicular to the oncoming flow (Figure 1). The stratification of the approach flow was kept neutral, whereas inside the cavity different buoyancy conditions were simulated by heating of the windward-facing wall. The boundary layer was simulated using vorticity generators and low density, flat plate roughness elements, with the resulting parameters of boundary layer height $\delta = 1$ m, displacement height $d = 0$ mm, and roughness length z_0 of between 1 and 1.6 mm, depending on the flow Reynolds number. The friction velocity u_*/U_{ref} varied between 0.064 and 0.070 over the freestream velocity range of 0.5 to 1 m s⁻¹. This

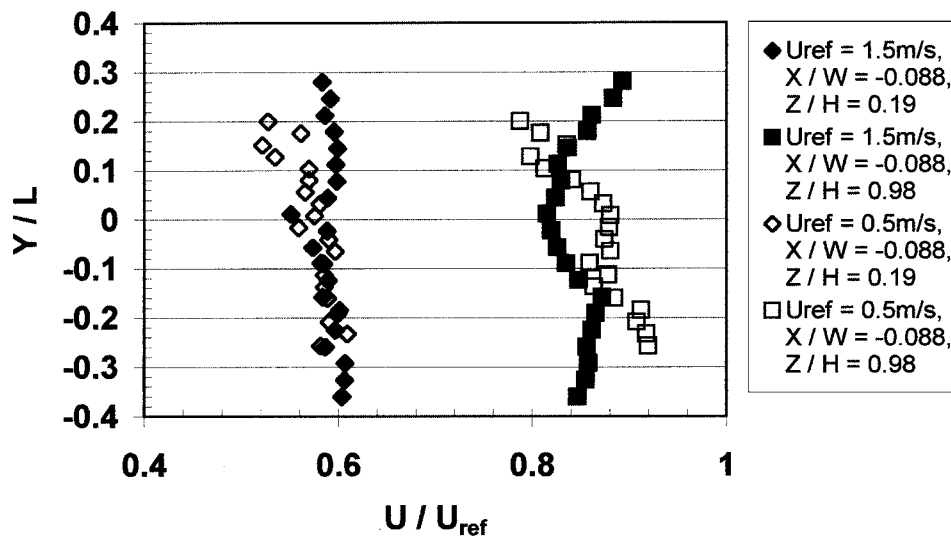


Figure 4. Spanwise variation of mean velocity in the boundary layer.

wind speed range gave canyon Reynolds numbers from 9.5×10^3 to 1.9×10^4 . The boundary layer profiles of mean velocity (\bar{U}) and turbulent kinetic energy (k) for this range of freestream speeds are shown in Figures 2 and 3, respectively, for two different locations upstream of the canyon, illustrating how the boundary layer was fully developed in all cases.

The velocity measurements were carried out with a two-component Laser-Doppler-Anemometer, with an accuracy of $\pm 3.5\%$ for the mean values and $\pm 4\%$ for the turbulence quantities. This includes the accuracy of the measurement system and the statistical error, as well as the repeatability of the measurements. The sampling frequency, dependent on the local flow seeding, was always at least 40 Hz inside the cavity (usually about 100 Hz) and typically 30 000 samples were taken per measurement point. The flow temperature measurements were taken with thermocouples (K-Type) and a Platinum-Resistance-Thermometer (PRT), with an accuracy of within $\pm 1.2^\circ$ for the thermocouples and $\pm 0.5^\circ\text{C}$ for the PRT.

The two-dimensionality both before and inside the cavity was established by the use of end plates that also enabled Reynolds number independence for the flow at velocities at or above 0.5 m s^{-1} . These end plates had a height of 0.8 m and they extended for distances of 4.5 and 2.4 m upstream and downstream of the canyon, respectively. Preliminary optimisation experiments showed that a spanwise spacing of $L = 2.5 \text{ m}$ between the end plates gave the highest degree of flow two-dimensionality. Hence, this setting was used in all the subsequent measurements, giving an effective spanwise aspect ratio of $L/W = 8.8$. Whilst this ratio is rather small for a nominally two-dimensional model it was considered that, for the purposes of this initial study, the most important factor was to optimise the quality of

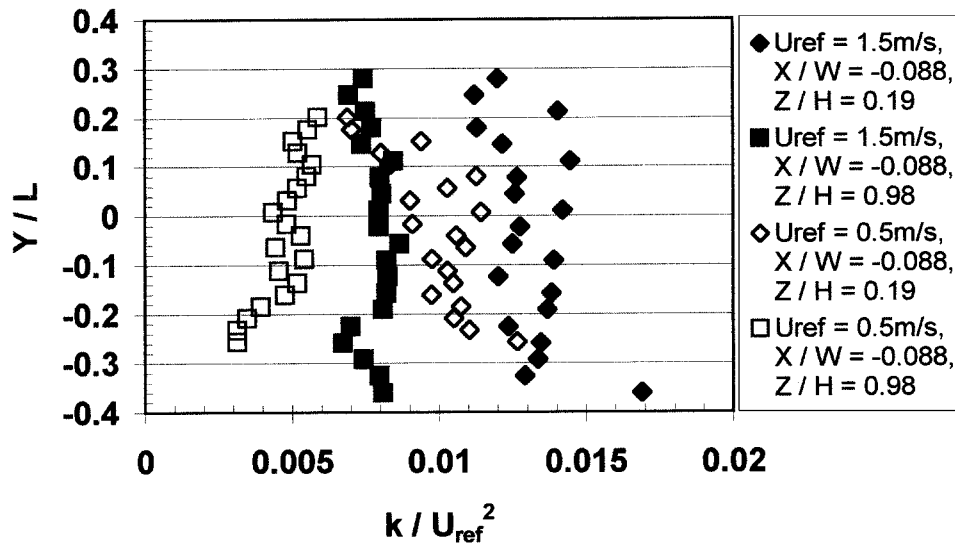


Figure 5. Spanwise variation of turbulent kinetic energy in the boundary layer.

the approach flow. At the two reference wind speeds examined, of 0.5 and 1.5 m s⁻¹, the lateral uniformity of the approach flow mean streamwise velocity and turbulent kinetic energy were within ± 5 and $\pm 10\%$, respectively, of their mean values measured over the central $\pm 20\%$ of the cavity length about the geometrical centre-plane, as illustrated in Figures 4 and 5.

The windward-facing wall was heated by heating mats, with the temperature being controlled via measurements from embedded thermocouples, whilst the other faces were cooled to ambient temperature. Although solar-induced wall heating is a complex issue, in this initial study only the differential temperature between the air and the heated wall was considered. A reasonable value for this is 5 °C (Sini *et al.*, 1996), although it will clearly vary with canyon geometry, cloud cover and time of day, for example. The thermal effect is only of potential importance at low wind speeds, certainly below 3 m s⁻¹ when the ‘urban dome’ regime is dominating. Hence, a simple canyon of 20 m height has been modelled subjected to full-scale wind speeds of 1–3 m s⁻¹. This gives Froude numbers of 0.27 to 2. In order to match this range the temperatures on the heated wall were established at either ambient (neutral case), 80 or 120 °C with the variation over the whole heated wall being within ± 5 °C of the mean value. The three different test velocities of 0.5, 0.8 and 1.0 m s⁻¹ (measured by a reference sonic anemometer located at a height of 1 m) resulted in Froude numbers ranging from 0.27 to 2.03 for the heated wall cases (the neutral case giving an infinite Froude number). Here, the Froude number has been defined as $Fr = U_{ref}^2 / (gH(T_w - T_{ref})/T_{ref})$, where T_w denotes the heated wall temperature, T_{ref} the ambient, freestream reference temperature (all temperatures in this expression are absolute values in Kelvin) and g the acceleration due to grav-

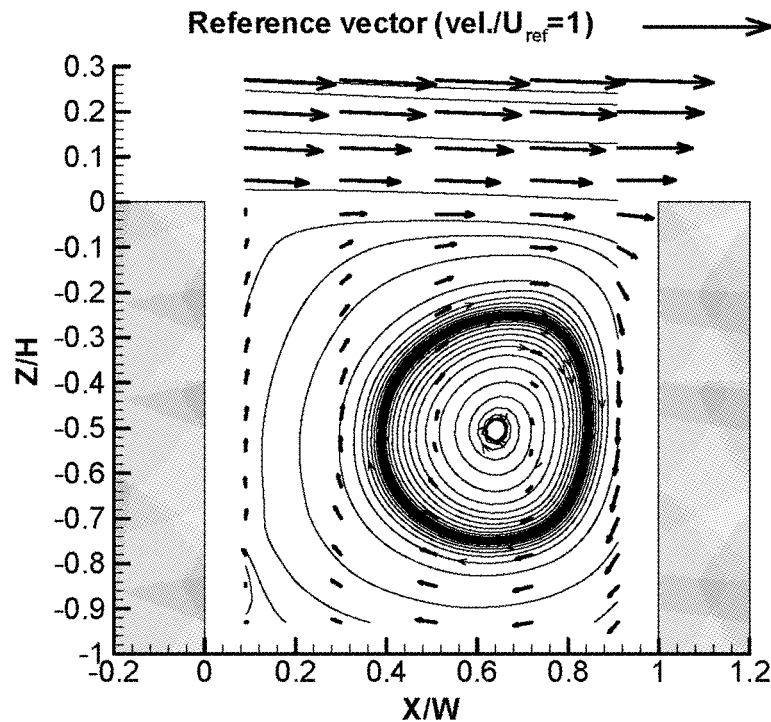


Figure 6. Projected mean velocity vectors and streampaths on canyon centre-plane. Neutral case, $U_{ref} = 1 \text{ m s}^{-1}$.

ity. Five vertical profiles of mean velocity and turbulence measurements were taken at the same streamwise locations, on the geometrical centre-plane, for all the different Froude number cases. Each profile commenced at 20 mm above the canyon base and extended into the shear layer where the data could be compared with the oncoming flow boundary layer conditions. At each position the time-histories of the streamwise (U) and vertical (W) velocity components were measured and the time-averaged velocity and turbulence statistics computed. Restrictions on the orientation of the LDA probe within the canyon flow regime prohibited the measurement of the third, lateral component of velocity (although, for completeness, these data were taken in the boundary layer). Hence, the turbulent kinetic energy (TKE) within the canyon was estimated as $k = 1/2(u'^2 + 2w'^2)$.

3. Results and Discussion

The projected mean velocity vectors on the centre-plane of the canyon, together with streampaths computed from these velocity distributions, are shown in Figures 6 to 10 for the neutral case through to the lowest Fr value. The figures for the heated wall cases also show the mean air temperature distributions. The influence

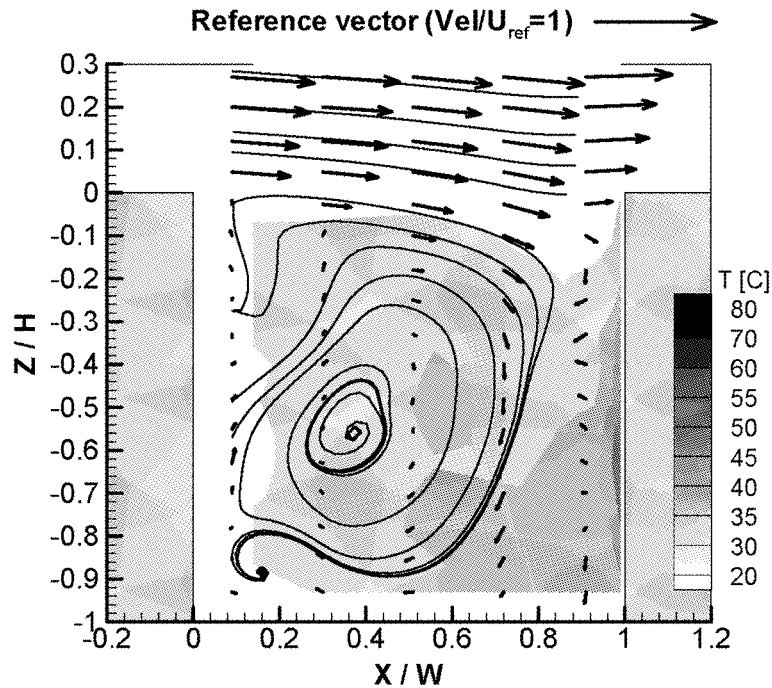


Figure 7. Projected mean velocity vectors, mean temperatures and streampaths on canyon centre-plane. $Fr = 2.03$, $U_{ref} = 1 \text{ m s}^{-1}$, $T_w = 80 \text{ }^\circ\text{C}$.

of the temperature due to the wall heating seems, in general, to be very small at the higher Fr cases examined. The overall feature of a single main vortex in the cavity remains for Fr down to 1.17, although the centre of the vortex tends to move slightly downwards and upstream with decreasing Fr value. For the lowest two Fr values a flow in the freestream direction, associated with a very weak secondary vortex, is found near the base of the canyon. This transition from a flow regime with single dominant vortex to one with a weaker secondary vortex close to the ground, that appears to take place at a Fr of the order of 1, is qualitatively, but not quantitatively, similar to the 2-D numerical predictions, using the code CHENSI (Sini *et al.*, 1996), for a geometrically similar cavity ($W/H = 1$) but with different approach flow conditions (Mestayer *et al.*, 1995). However, in their study this transition took place at a Fr value at least an order of magnitude higher. Further work is required, including direct comparisons of experiments and 3-D predictions of exactly the same test case, in order to explain these differences. However, it is to be expected that a 2-D prediction, with precisely defined and uniform heated wall temperature distributions, will yield different results from an experiment where there is variability in the wall heating and spanwise recirculations associated with the essential three-dimensionality of the configuration.

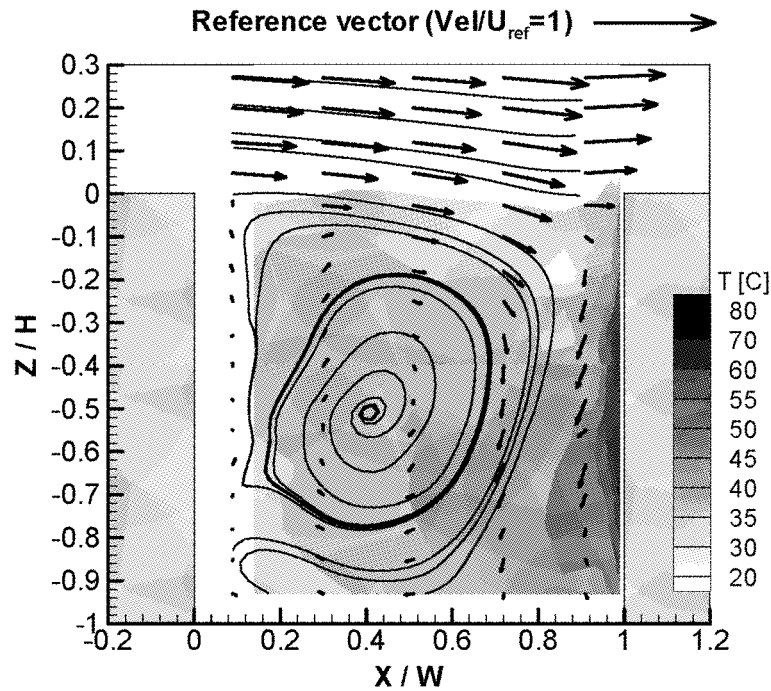


Figure 8. Projected mean velocity vectors, mean temperatures and streampaths on canyon centre-plane. $Fr = 1.17$, $U_{ref} = 1 \text{ m s}^{-1}$, $T_w = 120^\circ\text{C}$.

In all the cases examined there does not seem to be any evidence of an updraft close to the heated wall, even for the very lowest Fr regime. Since the profile nearest to the heated surface was taken at a distance of $0.09 W$ (25 mm) from the wall it is probable that there is a very thin layer close to the wall within which an updraft occurs. As part of a recent field experiment undertaken in a street in Nantes, France (Louka *et al.*, 2002), some flow visualisation was carried out using neutrally buoyant, helium-filled balloons (Vachon *et al.*, 1999). For wind directions perpendicular to the street axis balloons released at street level tended to remain within 5 m of the ground with no obvious tendency towards upwards or downwards motion, suggesting that they were trapped within the weak secondary vortex. However, those balloons that approached very close to the heated wall, so that they were almost touching the surface, always rose upwards along that wall and into the upper levels of the canyon.

In the present work the temperature distributions inside the canyon display some degree of similarity, except very close to the heated wall. Figures 11 to 14 show enlarged plots of the temperature distributions close to the heated wall for the range of Fr examined, in order to show more clearly the differences between the cases. The vertical location of the maximum temperature in the profile measured closest to the wall ($0.014 W$, or 4 mm, from the wall) changes significantly with Fr , from

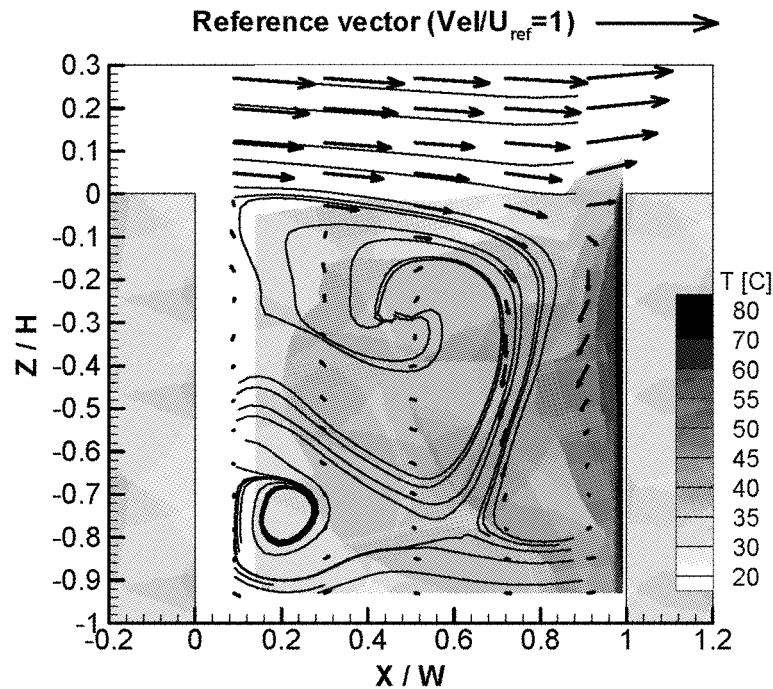


Figure 9. Projected mean velocity vectors, mean temperatures and streampaths on canyon centre-plane. $Fr = 0.73$, $U_{ref} = 0.8 \text{ m s}^{-1}$, $T_w = 120 \text{ }^{\circ}\text{C}$.

a position of $0.40 H$ above the canyon base at $Fr = 2.03$ and then $0.47 H$ at $Fr = 1.17$ to $0.82H$ at $Fr = 0.73$ followed by $0.75 H$ at $Fr = 0.27$. Thus, as with the mean velocity data, there appears to be a transition at $Fr \approx 1$. The value of the maximum temperature in each of these near-wall profiles increases with a decrease in Fr down to $Fr = 0.73$ and then decreases again at the lowest Fr examined. The profile shapes for the monotonic decrease of air temperature with distance from the heated wall are similar for all the Fr values, giving a thermal boundary layer thickness of the order of $0.2 W$, at those heights corresponding to the maximum near-wall temperature. Examining these plots, with those presented in Figures 6 to 10, clearly shows that the increase in height of the hottest region close to the heated wall is directly related to the weakening of the downwash associated with the dominant vortex. In addition, as the wall heating influence increases (decreasing Fr) and the main vortex weakens, along with the evolution of a region of stagnant flow beneath, the temperatures in the most upstream part of the canyon decrease. This indicates a reduced convection of the heat produced from the heated wall into this region.

Figures 15 to 19 show the distributions of TKE within and above the canyon for the different test conditions. It may be seen that for all the heated wall cases there is a significant increase in TKE near the heated wall. Given that the overall

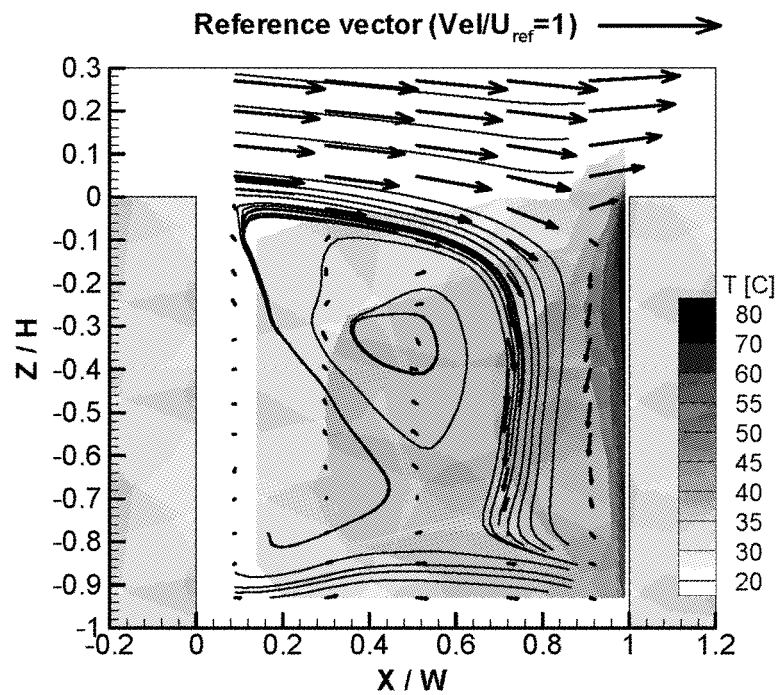


Figure 10. Projected mean velocity vectors, mean temperatures and streampaths on canyon centre-plane. $Fr = 0.27$, $U_{ref} = 0.5 \text{ m s}^{-1}$, $T_w = 120^\circ\text{C}$.

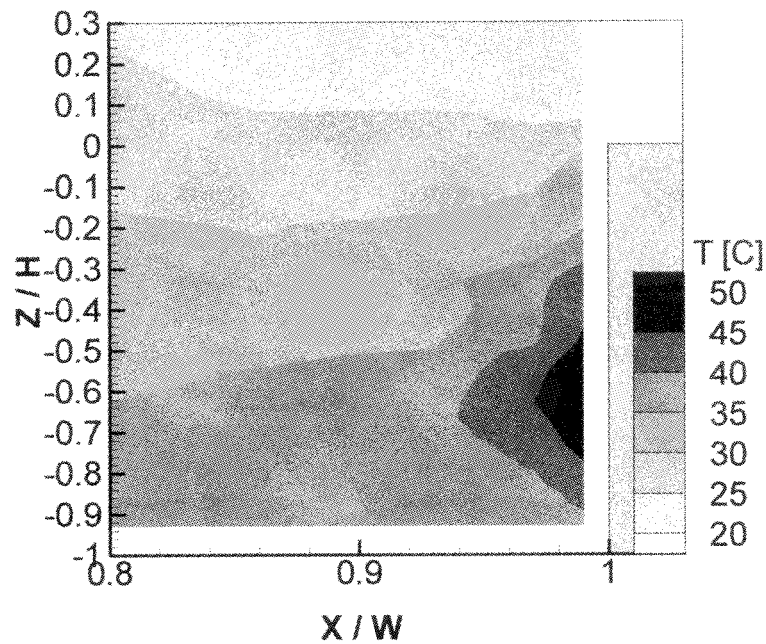


Figure 11. Detail of temperature distribution near heated wall for $Fr = 2.03$.

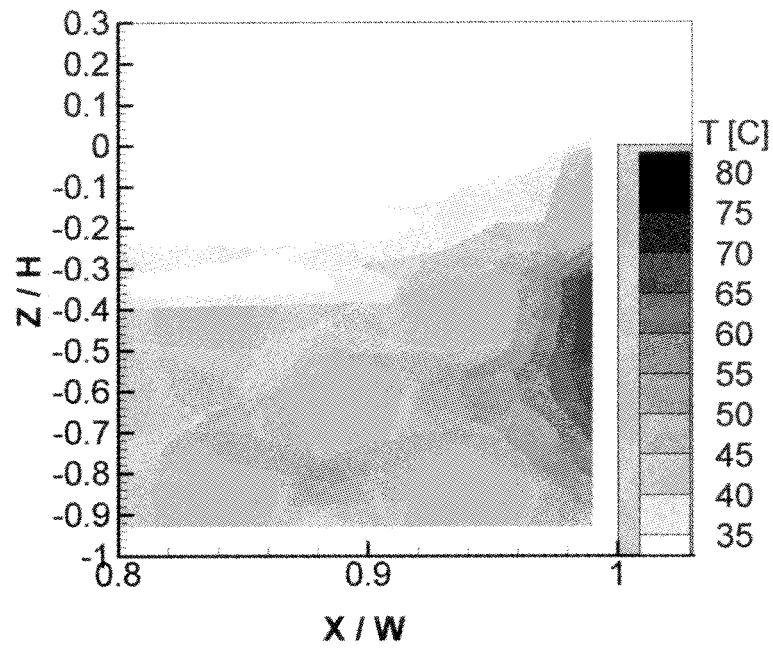


Figure 12. Detail of temperature distribution near heated wall for $Fr = 1.17$.

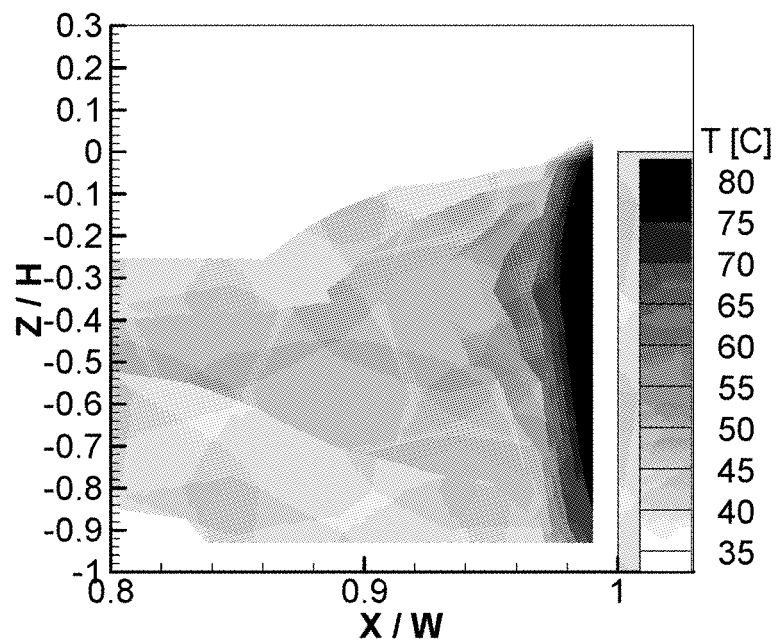


Figure 13. Detail of temperature distribution near heated wall for $Fr = 0.73$.

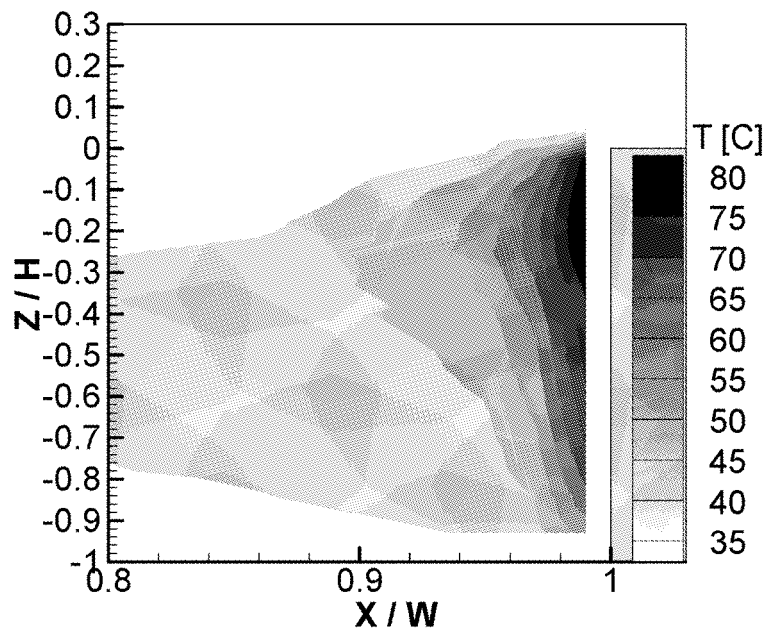


Figure 14. Detail of temperature distribution near heated wall for $Fr = 0.27$.

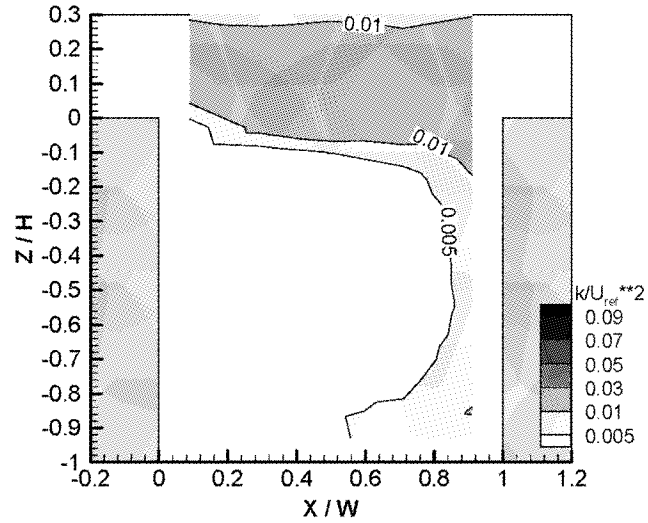


Figure 15. Distribution of turbulent kinetic energy in canyon for neutral case.

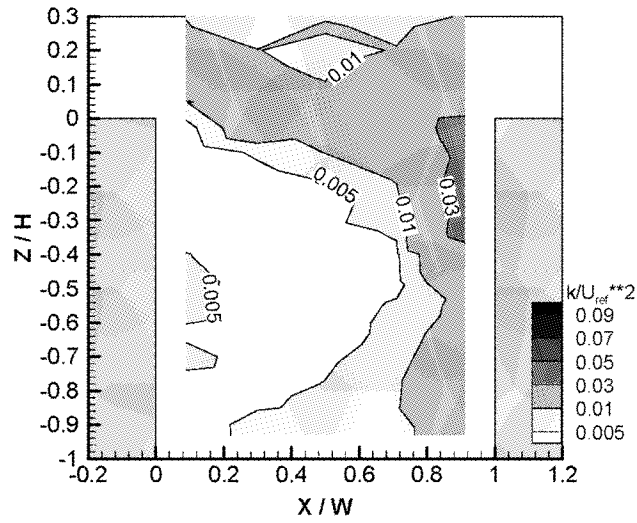


Figure 16. Distribution of turbulent kinetic energy in canyon for $Fr = 2.03$.

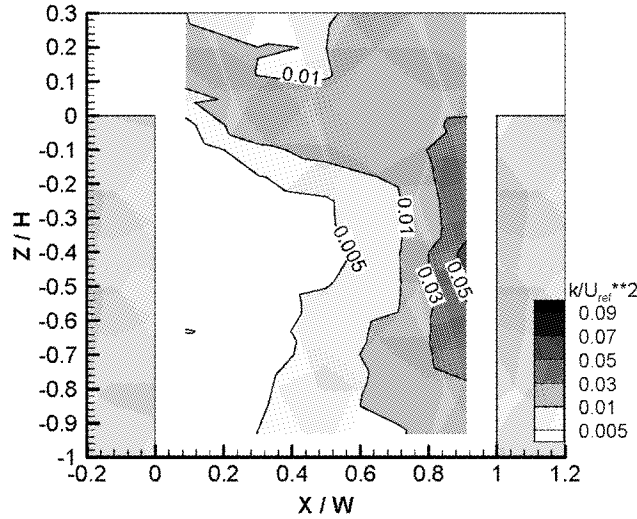


Figure 17. Distribution of turbulent kinetic energy in canyon for $Fr = 1.17$.

accuracy of the TKE measurements is $\pm 12\%$ the increase in TKE with decrease in Fr is always greater than this experimental uncertainty; neutral case ($Fr = \infty$), $k = 0.007 \pm 0.0008$; $Fr = 2.03$, $k = 0.03 \pm 0.004$; $Fr = 1.17$, $k = 0.05 \pm 0.006$; $Fr = 0.73$, $k = 0.07 \pm 0.008$; $Fr = 0.27$, $k = 0.11 \pm 0.013$. These are the maximum values measured in the profile closest to the wall, taken from each plot. Since there is probably insufficient shear in the mean flow in this region to produce such high TKE production, the primary source of production may be the high thermal

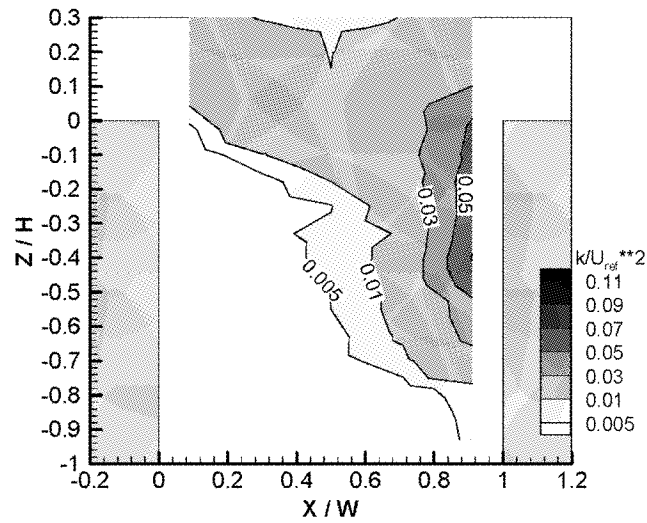


Figure 18. Distribution of turbulent kinetic energy in canyon for $Fr = 0.73$.

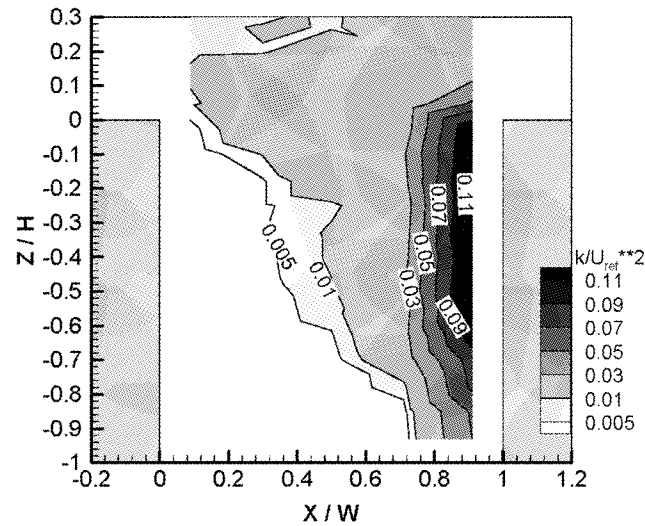


Figure 19. Distribution of turbulent kinetic energy in canyon for $Fr = 0.27$.

gradients near the wall. However, further measurements much closer to the heated wall would be required to verify the source of TKE production.

4. Concluding Remarks

The results from the present study indicate that the heating of the windward-facing wall does appear to have some influence on the generation of a very weak second-

ary flow close to the ground of the canyon at very low Froude numbers. However, so far there is little evidence that the buoyancy forces induce a widespread upward motion, except in a very thin layer near the heated wall, as also noted from field experiments in Nantes, France. Hence, it is not possible to clearly state that the effect of wall heating will be significant in terms of the canyon flow field and the motion and dispersion of pollutants. Further work is planned to examine the possible three-dimensionality of the canyon flow regime with wall heating, together with 3-D simulation, based on the CFD code CHENSI (Sini *et al.*, 1996), for predicting such flows.

Acknowledgements

The authors gratefully acknowledge funding from the EU within the TMR project TRAPOS (Contract ERBFMRXCT97-0105). The authors should also like to thank Dr. P. Hayden and Mr. T. Lawton from EnFlo and Mr. T. Renouf, Dr. P. Louka, Dr. P. G. Mestayer, and Mr. X. Mestayer from ECN for their contributions to this research.

References

- Albrecht, F.: 1933, 'Untersuchungen der vertikalen Luftzirkulation in der Grossstadt', *Meteorologische Zeitung* **50**, 93–98.
- DePaul, F. T. and Sheih, C. M.: 1986, 'Measurements of wind velocities in a street canyon', *Atmosph. Environ.* **20**, 555–559.
- Georgii, H. W., Busch, E. and Weber, E.: 1967, 'Untersuchung über die zeitliche und räumliche Verteilung der Immissions-Konzentration des Kohlenmonoxids in Frankfurt am Main', *Berichte des Instituts für Meteorologie und Geophysik der Universität Frankfurt am Main*, 11.
- Louka, P., Vachon, G., Sini, J.-F., Mestayer, P. G. and Rosant, J.-M.: 2002, 'Thermal effects on the airflow in a street canyon – Nantes'99 experimental results and model simulations', *Water, Air and Soil Pollut.*, this issue.
- Ludwig, F. L. and Dabberdt, W. K.: 1972, 'Evaluation of the APRAC-1A Urban Diffusion Model for Carbon Monoxide', *Final Report*, Coordinating Research Council contract CAPA-3-68 (1–69), NTIS No PD 2210819.
- Mestayer, P. G., Sini, J.-F. and Jobert, M.: 1995, 'Simulation of the Wall Temperature Influence on Flows and Dispersion within Street Canyons', in *Air Pollution '95, Vol. 1: Turbulence and Diffusion*, Porto Carras, Greece, September, pp. 109–106.
- Nakamura, Y. and Oke, T. R.: 1988, 'Wind, temperature and stability condition in an east-west-oriented urban canyon', *Atmosph. Environ.* **22**, 2691–2700.
- Ogawa, Y., Diosey, P. G., Uehara, K. and Ueda, H.: 1981, 'A wind tunnel for studying the effects of thermal stratification in the atmosphere', *Atmosph. Environ.* **15**, 807–821.
- Sini, J.-F., Anquetin, S. and Mestayer, P.: 1996, 'Pollutant dispersion and thermal effects in urban street canyons', *Atmosph. Environ.* **30**, 2659–2677.
- Uehara, K., Murakami, S., Oikawa, S. and Wakamatsu, S.: 1997a, 'Wind tunnel tests on stratified flow fields around urban street canyons by LDV', *J. Architect., Plann. Environ. Engineer. (Trans. of AIJ)* **492**, 39–46.

- Uehara, K., Murakami, S., Oikawa, S. and Wakamatsu, S.: 1997b, 'Wind tunnel test of concentration fields around street canyons within the stratified urban canopy layer', *J. Architect., Plann. Environ. Engineer. (Trans. of AIJ)* **499**, 9–16.
- Uehara, K., Murakami, S., Oikawa, S. and Wakamatsu, S.: 2000, 'Wind tunnel experiments on how thermal stratification affects flow in and above urban street canyons', *Atmosph. Environ.* **34**, 1553–1562.
- Vachon, G., Rosant, J.-M., Mestayer, P. G. and Sini, J.-F.: 1999, 'Measurements of Dynamic and Thermal Field in a Street Canyon. URBCAP Nantes'99', in *6th International Conference on Harmonisation within Atmospheric Dispersion Modelling for Regulatory Purposes*, Rouen, France, October 1999, 12 pp.
- Vachon, G.: 'Nantes'99', Internet-publication on <http://www.ec-nantes.fr/Fr/Recherche/DEE/Dah/gaelle.htm>.